Politecnico di Torino

Porto Institutional Repository

[Article] Opening angle of loose-snow avalanches

(Article begins on next page)
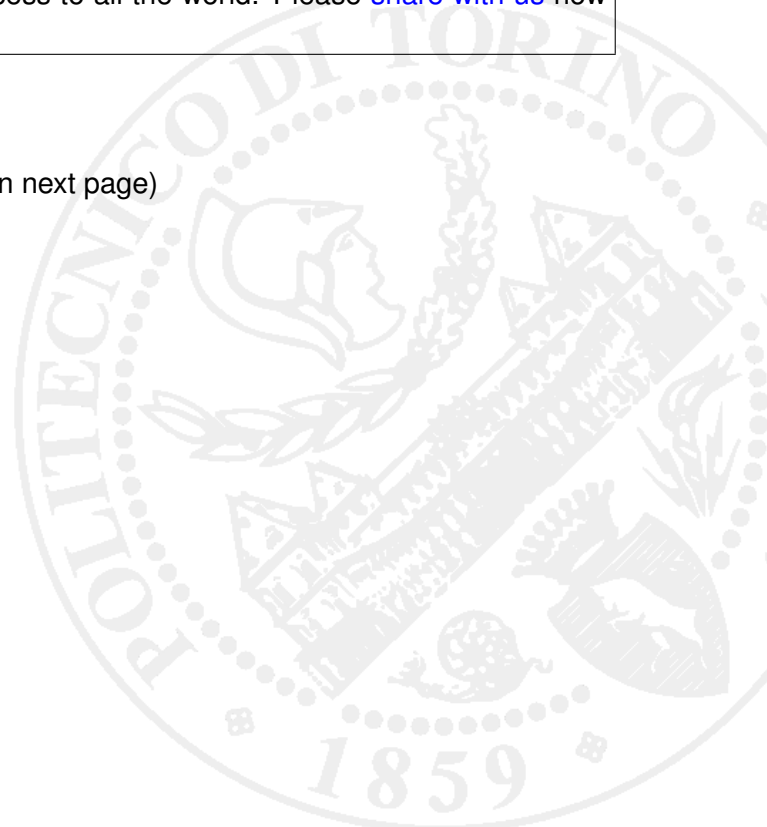
Opening angle of loose-snow avalanches

Valerio De Biagi*

* DISEG – Politecnico di Torino

1. Introduction

Loose-snow avalanches are well-diffused phenomena in mountain areas. Despite their frequency of occurrence, as the few literature available confirm, in the past, the researchers have not drawn attention to the phenomenon. On the contrary, the interest is held by slab avalanches that are more dangerous, large and responsible of most of the damages and fatalities (McClung and Schaerer, 2006; Maggioni and others, 2013; Barbero and others, 2013a). However, although loose-snow avalanches are smaller in size and interest smaller volumes of snow, they may be triggered in any period of the year: frequent are the cases in which alpinists are shot by discharges in high altitude ice faces or gullies in summer.

Loose-snow avalanches, or point avalanches, can form both in dry and wet snowpacks and are easy to recognise because of their shape (Schweizer and others, 2003). Differently from slab avalanches, where a fracture propagates in the snowpack (Chiaia and others, 2008) and large masses are involved in the initial movement, in loose-snow avalanches the initial volume is small, e.g. less than 10^4 m^3. A localised lack of cohesion in a small volume of snowpack implies that snow grains fold up on the underneath layers and start to move. The avalanche is triggered naturally when the slope angle exceeds the static-friction angle (or repose angle), named ϕ. Besides, the avalanche can be triggered by skiers even in thin layers of weak snow (Trautman and others, 2006).

Wet loose-snow avalanches are more frequent in late winter and in spring, dry loose-snow avalanches occur in newly fallen snow or in old surface snow that has faceted (Haegeli and others, 2010). Loose-snow avalanches can frequently take place during the snowy event: an intense snow precipitation with low density snowflakes presupposes low cohesion of the fresh snow and, therefore, small loose avalanches (discharges) happen if, as said, snow depth is larger than a critical value (Haefeli, 1967). Otherwise, a reduction of cohesion due to snowpack properties variation may trigger the avalanche. This is the case of metamorphosed snowpack in which there is a localised increase of snow temperature or water content. Often, the initiation is asso-

Loose-snow avalanches occur frequently after snow-falls or as long as snowpack evolves in winter. The two relevant points in the signature of this kind of avalanches are: the lack of internal cohesion and the inverted V shape of the avalanche, also known as "pear" shape. In this research paper, the opening angle of such snow avalanches is investigated. A discrete mechanical model is defined and Mohr-Coulomb yield criterion is considered. Thanks to a graphical solution that considers Mohr's circles, the opening angle is found and its independence from the value of the cohesion is shown.
Keywords: *loose-snow, loose-snow avalanche, mechanical model, Mohr, opening angle.*

Studio sull'angolo di apertura di valanghe di neve a debole coesione
Le valanghe di neve a debole coesione sono estremamente frequenti durante e subito dopo le nevicate (ossia in manti nevosi freschi), oppure possono verificarsi a seguito dell'evoluzione del manto nevoso durante la stagione invernale. Tali fenomeni naturali sono caratterizzati da due aspetti chiave: la mancanza di coesione nel manto nevoso e la forma a V rovesciata, talvolta detta "a pera". In questa nota tecnica, si fissa l'attenzione sull'angolo di apertura di tale di tipologia di valanghe. Per fare ciò, un modello meccanico in grado di discretizzare il manto nevoso ed il modello di resistenza di Mohr-Coulomb sono considerati. Grazie ad un approccio grafico basato sui cerchi di Mohr, l'angolo di apertura della valanga a debole coesione è definito così come è mostrata la sua indipendenza con il valore della coesione del manto nevoso.
Parole chiave: *valanga di neve, valanga di neve debole coesione, modello meccanico, Mohr, angolo di apertura.*

Etude sur l'angle d'ouverture d'avalanches de neige a faible cohesion
Les avalanches de neige à faible cohésion sont très fréquentes dans des dépôts de neige récente ou en cas de manteau neigeux qui a évolué pendant l'hiver. Deux traits distinguent ce genre de phénomènes naturels : l'absence de cohésion dans le manteau neigeux et la caractéristique forme a V, dite « à poire ». Dans ce document, l'angle d'ouverture de ce genre d'avalanches est étudié. Un modèle discret de la surface du manteau neigeux est mis en place. Le critère de résistance de Mohr-Coulomb est employé. L'approche graphique de Mohr est utilisée. L'angle d'ouverture de l'avalanche a faible cohésion résulte indépendant de la valeur de la cohésion même du manteau neigeux.
Mots clé: *avalanche de neige, avalanche de neige à faible cohésion, modèle mécanique, Mohr, angle d'ouverture.*
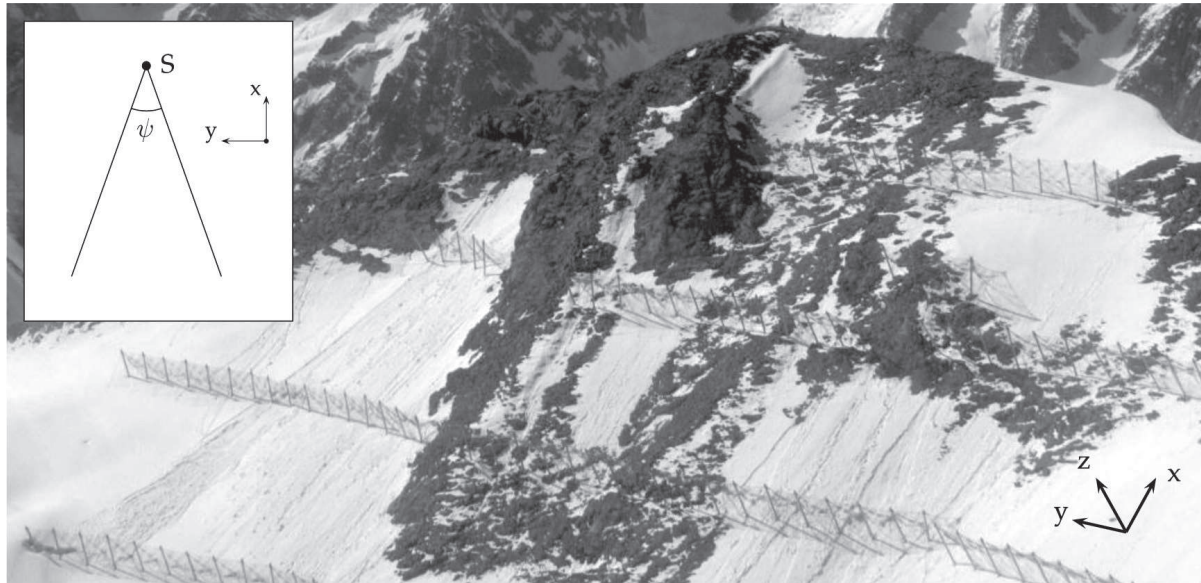
Fig. 1. Loose snow avalanches on the south face of Punta Liconi, Aosta Valley, Nortwestern Italian Alps. Image taken on May 22, 2007. The reference system plot in the figure refers to the conventions in the present paper. Loose-snow avalanches paths are clearly visible on the slope. The opening angle is defined with letter f and the starting point with letter S, see the box.
Valanga di neve a debole coesione sulla parete Sud della Punta Liconi, Valle d'Aosta. La fotografia è stata scattata il 22 maggio 2007. Il sistema di riferimento riportato sull'immagine si riferisce alle convenzioni riportate nel testo. I percorsi delle valanghe di neve a debole coesione sono chiaramente visibili sul pendio. Nel riquadro: l'angolo di apertura è denominato con la lettera ϕ e il punto di distacco è indicato con la lettera S.

ciated both to snowpack depth reduction around rock outcrops and to higher snow temperature (McClung and Schaerer, 2006).

The repose angle at which loose-snow avalanches trigger depends upon grain type and geometry. Dendritic crystals have high static-friction angle (up to 80°) and, as much as the grain turns into a round form the angle decreases to 35°. Moreover, the presence of water may further reduce the value of the angle. Slush snow may avalanche off of slopes of 15° or less (Roch, 1965; McClung and Schaerer, 2006). However, independently from snow type and causes, loose-snow avalanches are characterised by inverted V shape (triangle) with small opening angle, as the ones shown in Figure 1. The apex of the triangle is at the initiation point.

In the past, Haefeli (1967) studied the triggering conditions for loose-snow avalanches. He found that equilibrium conditions in the snowpack are broken if snow depth exceeds the critical value

$$h_0 = \frac{2c}{\gamma} \tan \left(\frac{\pi}{4} + \frac{\phi}{2} \right) \qquad (1)$$

where c and γ are snow cohesion and specific weight, respectively. His computations on stresses in the snowpack were made by means of graphical solutions based on the theory of Mohr's circles, a graphical way to solve stresses problems. It is interesting to notice that other authors used this approach in snow science because of its simplicity (Jaccard, 1966). Obviously, this ap-

proach is still used in geotechnics (Parry, 2004), where it was conceived.

One of the key aspects of the approach is the possibility to easily identify if a stress state is admissible for the material, i.e. no rupture occur. A stress state is not admissible, i.e. the material breaks, if the corresponding Mohr's circle is secant to the rupture envelope. The rupture envelope is defined empirically by means of laboratory tests and can be approximated by equations. In snow, the relationship between normal and shear stresses, σ and τ respectively, has been found to be accurately described by Mohr-Coulomb failure criterion, which yield line has the form

$$\tau = c + \mu\sigma \qquad (2)$$

where μ is the friction coefficient (Platzer and others, 2007), i.e. $\mu = \tan \phi$. This criterion is extensively applied in soil mechanics, for granular materials in static (Lancellotta, 2008) and dynamic conditions (Nedderman, 2005).

Besides that, the movement of granular materials plays an important role in many natural phenomena (Aranson and Tsimring, 2001), e.g. highly fractured rock masses movements; snow and ice avalanches are phenomena that can be studied in this framework (Savage and Hutter, 1991). Avalanche studies in layers of granular materials showed two types of behaviour, depending upon the thickness of the layer. Daerr and Dou-

ady (1999) showed that a perturbation on a thin layer of glass balls produces an avalanche propagating downhill and laterally, causing triangular tracks, similar to loose-snow avalanches. On the contrary, a perturbation on a thick layer produces an avalanche which propagates both downwards and upwards, with grains located uphill progressively tumbling down because loss of support. They assessed that the lateral propagation is due only to a small number of grains, which drive into motion some of their lateral neighbours. This chain process is repeated and the edges of the track are formed. Bouchaud and Cates (1998) proposed a simple interpretation of these observations based on an extension of a phenomenological model for surface flows.

Complex natural phenomena can be studied through simplified mechanical models that point on its features and bypass the physical details (De Biagi and Barbero, 2013). In this paper, a possible interpretation of loose-snow avalanches opening angle is given. The model, as shown, is based on a simple mechanical idea, which presupposes that a movement may affect not only the elements situated downhill, but also those situated laterally. The effects are transmitted with a friction mechanism. In order to explain clearly the results, a preliminary section on Mohr's circles construction and sign conventions is proposed. Then, the model is explained and commented. At the end, a parametric analysis is carried and results are discussed.

2. Summary on Mohr's circles

In this part, a brief summary on Mohr's graphical representation of stress states is proposed. These concepts are important for understanding the model described above.

Mohr (1900) first recognised the possibility to represent graphically a stress state on a special reference system $\sigma O \tau$, called stress space. His method provides a convenient graphical method for determining the normal and shearing stress on any plane through a point in a stressed body. The conventions used in what follows presuppose that (a) compressive stresses are positive and tensile stresses are negative, and (b) shear stresses are considered positive if they give a clockwise moment about a point above the stressed plane, otherwise negative (Murthy, 2002).

The normal stresses are taken as abscissae and the shear stresses as ordinates. For a given stress state represented by the stress tensor

$$[\sigma] = \begin{bmatrix} \sigma_x & \tau_{xy} \\ \tau_{xy} & \sigma_y \end{bmatrix} \tag{3}$$

it is possible to define and to plot on the stress space two points, P_1 and P_2 (see Figure 2), whose coordinates are

$$\begin{aligned} P_1 &= (\sigma_x; \tau_{xy}) \\ P_2 &= (\sigma_y; -\tau_{xy}) \end{aligned} \tag{4}$$

Stress state P1 acts on the vertical plane, while stress state P2 acts on the horizontal plane.

The mid-point of segment P_1P_2, named C, stays on the σ-axis at abscissa $(\sigma_x + \sigma_y)/2$, see Figure 2. The circle passing through the two points and centred in C has radius, r, equal to

$$r = \frac{1}{2}\sqrt{(\sigma_y - \sigma_x)^2 - 4\tau_{xy}^2}. \tag{5}$$

The two intersections between the circle and σ-axis have abscissae

$$\begin{aligned} \frac{\sigma_x + \sigma_y}{2} + \frac{1}{2}\sqrt{(\sigma_y - \sigma_x)^2 - 4\tau_{xy}^2} \\ \frac{\sigma_x + \sigma_y}{2} - \frac{1}{2}\sqrt{(\sigma_y - \sigma_x)^2 - 4\tau_{xy}^2} \end{aligned} \tag{6}$$

which are the eigenvalues of matrix $[\sigma]$, i.e. the principal stresses σ_1 and σ_3. The graphical solution is mainly used for finding the orientation of the principal planes if the normal and shear stresses on the surface of the prismatic element are known. The procedure considers a special point, called *origin of planes*, represented by point P_0 in Figure 2, which is the intersection between a vertical line conduced from point P_1, and a horizontal line conduced from P_2. The lines joining point P_0 with the intersections of the circle with σ-axis are the directions associated with the principal stresses.

Moreover, it is possible to find, given a rupture envelope in the stress space, the value of the rupture angle of the specimen. Considering the reference system made by the directions, which correspond to the principal stresses, the rupture angle is the angle formed by the line joining the
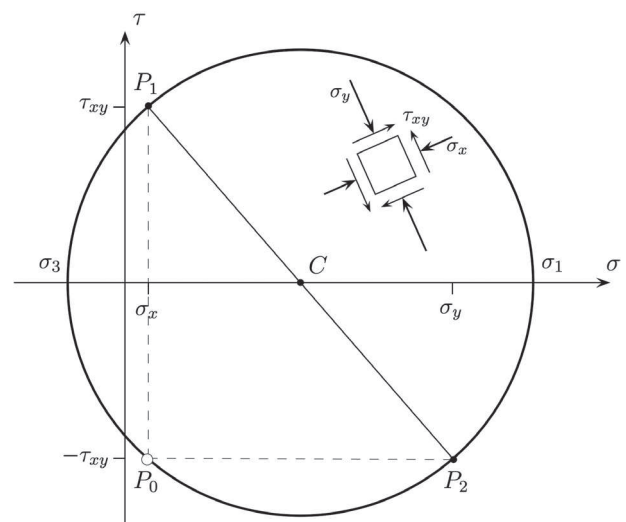
Fig. 2. Graphical representation of the stress tensor $[\sigma]$.
Rappresentazione grafica del tensore delle tensioni $[\sigma]$.

origin of planes and the tangency point between the circle and the rupture envelope. More details can be found further in the article and in Parry (2004).

3. Stresses in a uniform snowpack

The distribution of stresses in natural snow slabs has been studied in the past (Jaccard, 1966; Haefeli, 1967). The slab central region, where slope parallel gradients are approximately zero and where stress metamorphosis has a stabilising effect, is called *neutral zone* (Perla, 1975). The snowpack is modelled as an infinitely extended layer inclined to the horizontal at an angle of θ. Locally, the snowpack is considered uniform in thickness, H, and material properties, elastic modulus, E, and Poisson's ratio, ν. A coordinate system is set on snow surface, see Figure 3.

The equilibrium equations, which consider the six components of the stress tensor, can be expressed as

$$\begin{cases} \dfrac{\partial \sigma_x}{\partial x} + \dfrac{\partial \tau_{xy}}{\partial y} + \dfrac{\partial \tau_{xz}}{\partial z} + \mathcal{F}_x = 0 \\[2mm] \dfrac{\partial \tau_{xy}}{\partial x} + \dfrac{\partial \sigma_y}{\partial y} + \dfrac{\partial \tau_{yz}}{\partial z} + \mathcal{F}_y = 0 \\[2mm] \dfrac{\partial \tau_{xz}}{\partial x} + \dfrac{\partial \tau_{yz}}{\partial y} + \dfrac{\partial \sigma_z}{\partial y} + \mathcal{F}_z = 0 \end{cases} \quad (7)$$

where $\mathcal{F}_i$ are the components of the volume force along the axes,

$$\begin{cases} \mathcal{F}_x = -g\rho \sin \theta \\ \mathcal{F}_y = 0 \\ \mathcal{F}_z = -g\rho \cos \theta \end{cases} \quad (8)$$

g is the acceleration of gravity (9.81 ms^{-2}) and ρ is the local density of the snowpack. In the hypotheses of infi-
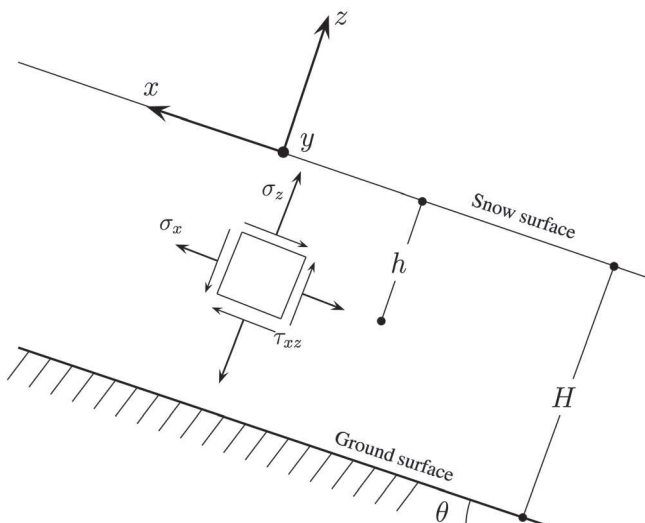

Fig. 3. Definition of snowpack reference system, sizes and forces. *Definizione del sistema di riferimento, delle dimensioni e delle tensioni del manto nevoso.*

nite slope, the partial derivatives with respect of x and y are null. The equilibrium equations simplify in

$$\begin{cases} \dfrac{\partial \tau_{xz}}{\partial z} = g\rho \sin \theta \\[2mm] \dfrac{\partial \tau_{yz}}{\partial z} = 0 \\[2mm] \dfrac{\partial \sigma_z}{\partial z} = g\rho \cos \theta \end{cases} \quad . \quad (9)$$

The dilatations along x and y axes, ε_x and ε_y, respectively, are null. Supposing the material linear elastic and isotropic,

$$\begin{aligned} \varepsilon_x = 0: \quad & \sigma_x - \nu(\sigma_y + \sigma_z) = 0, \\ \varepsilon_z = 0: \quad & \sigma_z - \nu(\sigma_y + \sigma_x) = 0. \end{aligned} \quad (10)$$

In the same manner, the distortions on xy and yz planes, γ_{xy} and γ_{yx}, respectively, are null. Within the same hypotheses,

$$\begin{aligned} \gamma_{xy} = 0: \quad & \tau_{xy} = 0, \\ \gamma_{yz} = 0: \quad & \tau_{yz} = 0. \end{aligned} \quad (11)$$

The integration of the previous eqs. (9), (10) and (11), leads to the following solution:

$$\begin{aligned} \sigma_x &= \frac{\nu}{1-\nu}\sigma_z \\[2mm] \sigma_y &= \frac{\nu}{1-\nu}\sigma_z \\[2mm] \sigma_z &= \cos \alpha \int_{-h}^{0} g\rho\, dz \\[2mm] \tau_{xy} &= 0 \\[2mm] \tau_{xz} &= \sin \alpha \int_{-h}^{0} g\rho\, dz \\[2mm] \tau_{yz} &= 0 \end{aligned} \quad (12)$$

where h is the depth of the point in which the stresses are computed ($0 < h < H$). In case of purely elastic case, ν is Poisson's ratio (Perla, 1975). In case of purely viscous case, ν is the viscous analogue of Poisson's ratio (Perla, 1973). The term $\nu / (1-\nu)$ can be related to creep angle, and consequently, to the density (Haefeli, 1963).

Substituting $h = 0$ in the previous eqs. (12), the stress state on snow surface is computed:

$$\begin{aligned} \sigma_x = \sigma_y = \sigma_z = 0, \\ \tau_{xy} = \tau_{xz} = \tau_{yz} = 0. \end{aligned} \quad (13)$$

4. A discrete model for damage propagation in a loose snowpack

In this section, a novel model for triggering propagation, focusing on the opening angle in loose snow avalanches, is described and analysed. The discretisation

of snowpack surface through simple shapes and mutual contact, leads to a propagation model, which, in some ways, may relate to domino effect, i.e. a cumulative effect is produced when one event sets off a chain of similar events (Stronge, 2004).

Let us consider the uppermost layer constituting the snowpack as a series of small elements (of infinitesimal dimensions) laying on the underneath layers (which are not considered for the moment). A sketch of the model is represented in Figure 4. Each element in the model is able to transmit its action to its neighbour elements with normal pressure (along the columns) or shear (along the rows).

Supposing that the avalanche triggers in element A of Figure 4, since the internal cohesion reduces, the self weight of the particle cannot be transmitted to the underneath layers. Self-weight of element A is turned into a normal pressure on element B and into a shear stress on elements C_1 and C_2. As a matter of evidence, we suppose that the point avalanche spreads laterally if the actions are larger than the corresponding internal resistances.

Since the purpose of the note does not relate to loose snow avalanche triggering, no requirements are need for the initial mechanism. In this sense, one may suppose that the elements interact in a complex manner and the failure might be due to evolving critical stages in the neighbouring elements, as proposed by Bak and others (1988). As stated, the effort of this simple research is devoted to the analysis of the opening angle.

The propagation mechanism remains in the xy initial plane. The stress tensor on the surface of the snowpack is null, see the previous section. This state can be represented on $\sigma\tau$-stresses plane with a point centred in the origin (i.e. a circle with radius equal to zero). In case of normal pressure (as the case of element B), the original Mohr state turns into a circle passing per the origin and point N_1, representing σ_x value, as represented in left-hand side of Figure 5. On the contrary, in case of shear (as the case of elements C_1 and C_2), Mohr state is a circle centred in the origin with radius τ_{xy} as represented in right-hand side of Figure 5. The new stress states can be admissible or not, depending if the circle is internal or secant to the yield bounds. Plain circles of Figure 5 refer to admissible stress states, dotted circles to non-admissible stress states.

For the analysis of the lateral spread of the effects of the triggering of a point avalanche, it is necessary to work on the evolution of the stress state of elements C_1 and C_2. At the initial stage, as already stated, a point centred in the origin represents the stress state. Since the tangential stress τ_{xy} increases, the stress state can be expressed by a circle centred in the origin with radius r. As much as the value of τ_{xy} increases, i.e. the radius of
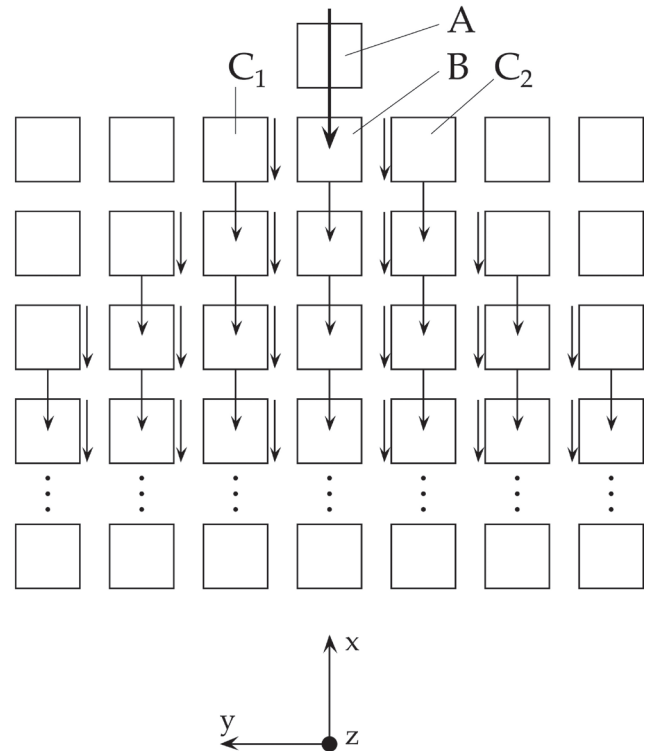

Fig. 4. A sketch of the discrete domino model. The top element starts to move and its action is transmitted via direct pressure or friction to the neighbour elements generating a chain reaction.
Rappresentazione del modello discreto. L'elemento sommiate inizia a muoversi e la sua azione è trasmessa agli elementi limitrofi tramite un'azione diretta o uno sfregamento. Si realizza quindi un'azione a catena.

the circle increases, the circle is more and more close to the rupture envelope. For a given value τ^*_{xy}, Mohr's circle is tangent to the rupture envelope in point R, see Figure 6.

The stress state at this precise point is now analysed and the rupture angle is found. Considering element C_2, the stress condition at the moment of rupture is shown in Figure 6. For the sign conventions, τ_{xy} referred to the face orthogonal to x-axis is negative, while τ_{xy} referred to the face orthogonal to y-axis is positive. The initial points for tracing the circle are

$$P_1 = \left(0; -\tau^*_{xy}\right)$$
$$P_2 = \left(0; \tau^*_{xy}\right). \tag{14}$$

The origin of planes, P_0, is found by tracing an horizontal line (a parallel to the plane with normal identified by x-axis) from P_1 and a vertical line from P_2 (idem, with y-axis). Point P_0 coincides with point P_1. The principal stresses, σ_1 and σ_3, and the directions identifying the principal reference system are found, plain grey lines in Figure 6. The principal reference system is rotated anti-clockwise of an angle of 45°. Supposing to consider
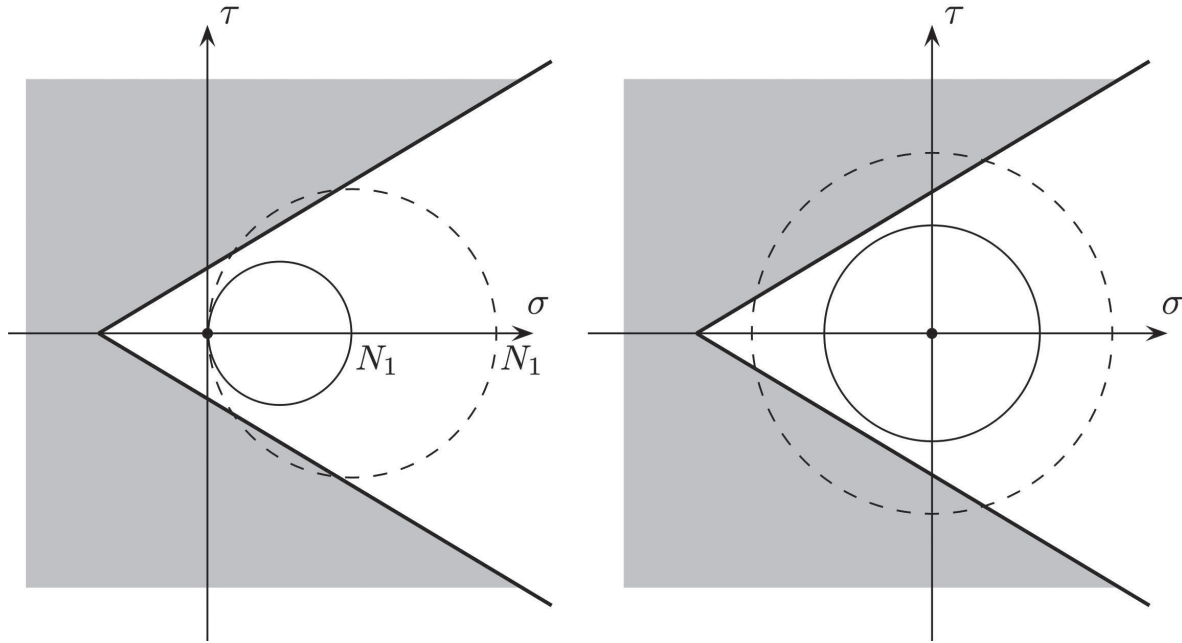
Fig. 5. Effects of normal pressure (left-hand side sketch) and shear (right-hand side) on a null stress state. The original stress state is represented by the point in the origin of the axes. Grey shaded area represents the non-admissible points, the bounds of Mohr-Coulomb yield criterion, i.e. the points for which $|\tau| > c + \mu\sigma$. Plain circles represent admissible stress states, while dotted circle represent non-admissible stress states. Compressions are positive.

Effetti di una pressione nomale (grafico di sinistra) e di una tangenziale (grafico di destra) agenti su un corpo scarico. Lo stato di tensione iniziale è rappresentato del punto nell'origine degli assi. L'area grigia rappresenta gli stati tensionali non ammissibili, ovvero i punti esterni al dominio di rottura di Mohr-Coulomb (quelli per cui si ha $|\tau| > c + \mu\sigma$). I cerchi in linea continua si riferiscono a stati di tensione ammissibili, mentre quelli in linea tratteggiata a strati di tensione non ammissibili. Le compressioni sono positive.
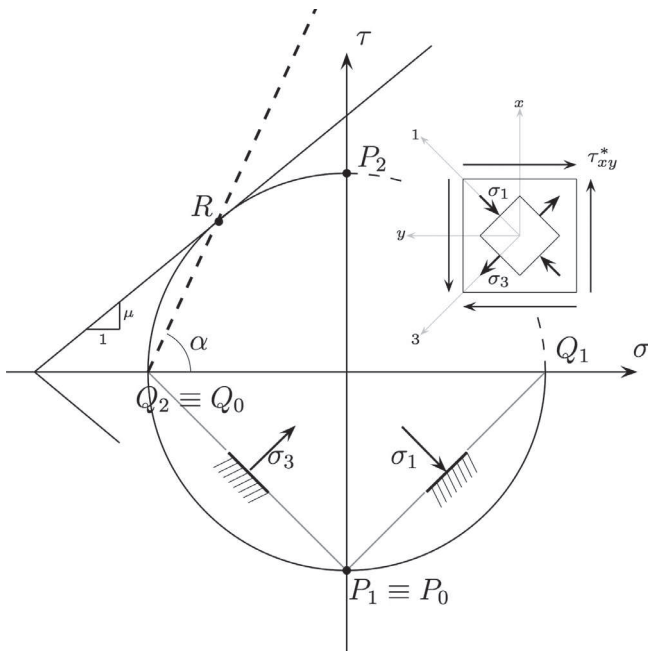

Fig. 6. Stress condition on element C_2 at the moment of rupture. Points P_1 and P_2 refer to reference system xy; points Q_1 and Q_2 refer to reference system 13. The thick dashed line represents the rupture plane in the principal reference system 13.
Stato tensionale sull'elemento C_2 nell'istante di rottura. I punti P_1 e P_2 si riferiscono al sistema di riferimento xy; i punti Q_1 e Q_2 si riferiscono al sistema di riferimento 13. Il tratteggio spesso rappresenta il piano di rottura nel sistema di riferimento principale 13.

the stresses in the principal reference system, the points identifying Mohr's circle are

$$Q_1 = (\sigma_1; 0)$$
$$Q_2 = (\sigma_3; 0).$$

(15)

Therefore, it is possible to find the new origin of planes, Q_0, with the same procedure previously described.

It is now possible to repeat the same reasoning in the principal reference system. The origin of planes, Q_0, is found to be coincident with point Q_2. The tangency point between Mohr's circle and the rupture envelope, as previously stated, is named with letter R, see Figure 6. The line Q_0R represents the rupture plane, with inclination α, in reference to the plane on which the greater principal stress acts, i.e. σ_1.

Being the relationship between friction coefficient and friction angle

$$\mu = \tan\phi$$

(16)

the rupture angle is now investigated. The angle ϕ represents the inclination of the rupture envelope with respect to σ-axis.

Consider the triangle ΔMRO of Figure 7: segment $\overline{MR}$ is perpendicular to segment $\overline{RO}$, because of the tangency between the rupture envelope and Mohr's circle.
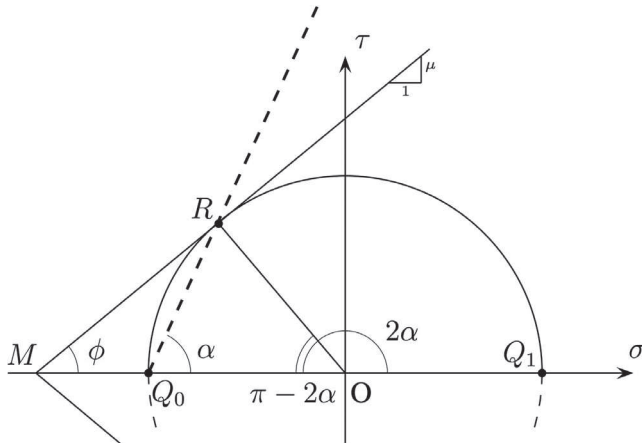
Fig. 7. Stress condition on element C_2 at the instant of rupture. This is a detail of Figure 6 with indications of the geometry and of the angles used in the text.
Stato tensionale sull'elemento C_2 nell'istante di rottura. Questo è un dettaglio della Figura 6 con le indicazioni della geometria e degli angoli utilizzati nel testo.
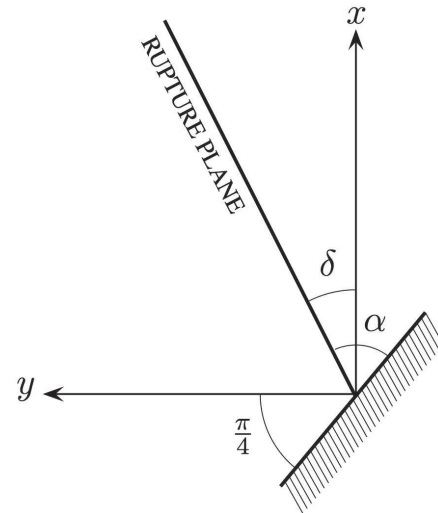

Fig. 8. Geometrical definition of the opening angle of the loose-snow avalanche.
Determinazione geometrica dell'angolo di apertura della valanga di neve a debole coesione.

For a geometry theorem on circles and triangles, which states that an angle inscribed in a circle is half of the central angle that subtends the same arc on the circle,

$$\angle ROQ_1 = 2 \angle RQ_0Q_1 = 2\alpha. \qquad (17)$$

Angles $\angle ROQ_1$ and $\angle ROQ_0$ are supplementary, therefore

$$\angle ROQ_0 = \pi - 2\alpha. \qquad (18)$$

Since the sum of the internal angles of a triangle is equal to a straight angle (π), the following expression can be applied to triangle ΔMRO,

$$\phi + \frac{\pi}{2} + \pi - 2\alpha = \pi. \qquad (19)$$

Thus, the relationship between the rupture angle, α, and the friction angle, ϕ, can be written

$$\alpha = \frac{\phi}{2} + \frac{\pi}{4}. \qquad (20)$$

Considering that the plane on which the principal stress, σ_1, acts is rotated 45° anti-clockwise, the angle between x-axis and the rupture plane is

$$\delta = \alpha - \frac{\pi}{4} = \frac{\phi}{2}, \qquad (21)$$

as can be seen in Figure 8.

As found, the rupture plane is inclined of an angle δ with respect to x-axis, i.e. the direction parallel to avalanche track. The same phenomenon may be related to element C_1, which is symmetric to the one considered above with respect to the vertical direction. At the apex

of the avalanche, i.e. the triggering point, the two rupture planes form an angle of 2δ, which is the opening angle. As a first outcome of the previous analysis, the opening angle is affected only by the value of the friction angle, not by the cohesion of the material. This aspect is important, as much as the fact that slope geometry does not enter in the expression of the opening angle. This fact may explain the observed fact that geometrically similar loose-snow avalanches occur in the same area, independently from slope characteristics.

5. Conclusions

Since no systematic studies have been conduced on loose-snow avalanches, few considerations on the capabilities of the model are made. Its effectiveness is, thus, based on simple observations and on the values assumed by the friction angle, ϕ, as found in literature (Roch, 1965; McClung and Schaerer, 2006).

As a geometric construction, δ-angle and half of the opening angle, $\psi/2$, are alternate interior angles, and, because x-axis coincides with the vector gradient of snow surface, the two angles are equal. Therefore, the opening angle of the loose-snow avalanche is

$$\psi = 2\delta = \phi. \qquad (22)$$

Following this result, the greater the friction angle, the greater the opening angle.

Classifying the snow for its water content, the following distinction can be made. In dry disaggregated snow, the friction angle depends on the shape of the

grains. Angle ϕ is about 35° in case of rounded forms and can increase up to 80° for dendritic crystals. On the contrary, in wet snow, the value of the friction angle is influenced by water content: ϕ reduces as much as water content approaches to saturation.

Independently from that, the common friction angle that can characterise the snow of point avalanches ranges from 20° to 40°. This fact implies that the computed opening angle ranges, as well, between 20° and 40° (Roch, 1965; McClung and Schaerer, 2006).

Although this result is preliminary, the model seems to centre the observed, but never recorded and classified, values. Despite the presence of a limited literature on the topic, the evaluation of the opening angle has important implications in the risk analysis. In particular, it can be useful for the computation of the area affected by the avalanche and, consequently, for locating the elements at risk. In fact, it gives indications about the possibility of interaction between a loose-snow avalanche and constructions, such masts, electric poles or buildings, and infrastructures. The spatial variability can be taken into account in decision tools on road management (Zischg and others, 2005).

As shown, the opening angle strictly depends on the friction angle of the snow. In the future, experimental studies would be conduced directly on the snowpack in order to get accurate measures of this parameter and its correlation with snow density, slope exposure, and meteorological conditions (Barbero and others, 2013b). Moreover, in order to support this study, a detailed and extended survey on real loose-snow avalanches has to be planned. In this case, opening angles and local topography can be estimated with aerial photogrammetrical photos and surveys onsite.

References

Aranson, I.S. e Trimring, L.S., 2001. Continuum description of avalanches in granular media. Phys. Rev. E, 64, 020301, doi: 10.1103/PhysRevE.64.020301.

Bak, P., Tang, C. e Wiesenfeld, K., 1988. Self-organized criticality. Phys. Rev. A, 38, 364-374.

Barbero, M., Barpi, F., Borri-Brunetto, M., Bovet, E., Chiaia, B. De Biagi, V., Frigo, B., Pallara, O., Maggioni, M., Freppaz, M., Ceaglio, E., Godone, D., Viglietti, D. e Zanini, E., 2013a. A new experimental snow avalanche test site at Seehore peak in Aosta Valley (NW Italian Alps) — Part II: Engineering aspects. Cold Regions Science and Technology, 86, 14-21.

Barbero, M., Barpi, F., Borri-Brunetto, M. e Pallara, O., 2013b. An apparatus for in-situ direct shear tests on snow. Experimental Techniques, doi: 10.1111/ext.12046.

Bouchaud, J.P. e Cates, M.E., 1998. Triangular and uphill avalanches of a tilted sand-pile. Granular Matter, 1, 101-103, doi:10.1007/s100350050015.

Chiaia, B., Cornetti, P. e Frigo, B., 2008. Triggering of dry snow slab avalanches: stress versus fracture mechanical approach. Cold Regions Science and Technology, 53, 170-178.

Daerr, A. e Douady, S., 1999. Two types of avalanche behaviour in granular media. Nature, 399, 241-243, doi:10.1038/20392.

De Biagi, V. e Barbero, M., 2013. Sviluppo di un modello meccanico per l'analisi del crollo di seracchi di ghiaccio. Geoingegneria Ambientale e Mineraria, L, 19-26.

Haefeli, R., 1963. Stress transformations, tensile strengths, and rupture processes of the snow cover. In: W.D. Kingery (Editor), Snow and Ice: Properties, Processes, and Applications, 560-575.

Haefeli, R., 1967. Some mechanical aspects on the formation of avalanches. In: H. Oura (Editor), Physics of Snow and Ice, 1, 1200-1213.

Haegeli, P., Atkins, R. e Klassen, K., 2010. Auxiliary material for Decision making in avalanche terrain: a field book for winter backcountry users. Canadian Avalanche Centre, Revelstoke, B.C.

Jaccard, C., 1966. Stabilité des plaques de neige. [Union Géodésique et Géophysique Internationale. Association Internationale des Sciences Hydrologiques. Commission des Neiges et Glaces.] Symposium International sur les aspects scientifiques des avalanches de neige, Davos, 170-181, IAHS-AISH Publication No. 69.

Lancellotta, R., 2008. Geotechnical Engineering. Taylor & Francis.

Maggioni, M., Freppaz, M., Ceaglio, E., Godone, D., Viglietti, D., Zanini, E., Barbero, M., Barpi, F., Borri-Brunetto, M., Bovet, E., Chiaia, B., De Biagi, V., Frigo, B. e Pallara, O., 2013. A new experimental snow avalanche test site at Seehore peak in Aosta Valley (NW Italian Alps) part I: Conception and logistics. Cold Regions Science and Technology, 85, 175-182.

McClung, D. e Schaerer, P., 2006. The Avalanche Handbook. The Mountaineers. Mohr, O., 1900. Die Elastizitatsgrenze Und Bruseheines Materials (The elastic limit and the failure of a Material). Zeitschrift Veneins Deuesche Ingenieure, 20, 1524-1530 + 1572-1577.

Murthy, V.N.S., 2002. Geotechnical Engineering: Principles and Practices of Soil Mechanics and Foundation Engineering. Marcel Dekker Inc.

Nedderman, R.M., 2005. Statics and Kinematics of Granular Materials. Cambridge University Press.

Parry, R.H., 2004. Mohr Circles, Stress Paths and Geotechnics. Taylor & Francis.

Perla, R.I., 1973. Hyperbolic stress equations for compressible slabs. Int. J. Non-Lin. Mech., 8, 253-259.

Perla, R.I., 1975. Stress and fracture of snow slabs.

[Union Géodésique et Géophysique Internationale. Association Internationale des Sciences Hydrologiques. Commission des Neiges et Glaces.] Symposium. Mécanique de la Neige. Actes du colloque de Grindelwald, Avril 1974, 208-221, IAHS-AISH Publication No. 114.

Perla, R.I. e Lachapelle, E.R., 1970. A theory of snow slab failure. J. Geophys. Res., 75, 7619-7627.

Platzer, K., Bartelt, P. e Kern, M., 2007. Measurements of dense snow avalanche basal shear to normal stress ratios (S/N), Geophys. Res. Lett., 34, L07501, doi:10.1029/2006GL028670.

Roch, A., 1965. An approach to the Mechanism of Avalanche Release. The Alpine Journal, 70, 57-68.

Savage, S. e Hutter, K., 1991. The dynamics of avalanches of granular materials from initiation to runout. Part I: Analysis. Acta Mechanica, 86, 201-223, doi: 10.1007/BF01175958.

Stronge, W.J., 2004. Impact Mechanics. Cambridge University Press.

Schweizer, J., Bruce Jamieson, J. e Schneebeli, M., 2003. Snow avalanche formation. Rev. Geophys., 41, 1016, doi:10.1029/2002RG000123.

Trautman, S., Lutz, E., Birkeland, K.W. e Custer, S.G., 2006. Relating wet loose snow avalanching to surfacial shear strength. In: Proceedings of the 2006 International Snow Science Workshop, Telluride, Colorado, 71-78.

Zischg, A., Fuchs, S., Keiler, M. e Meissl, G., 2005. Modelling the system behaviour of wet snow avalanches using an expert system approach for risk management on high alpine traffic roads. Natural Hazards and Earth System Science, 5, 821-832.